JOURNAL OF MATERIALS SCIENCE 19 (1984) 2172–2182

Microstructures and superconducting properties of *in situ* V_3Ga composite prepared by external diffusion process

T. TAKEUCHI, K. TOGANO, K. TACHIKAWA
National Research Institute for Metals, 1-2-1, Sengen, Sakura-mura, Niihari-gun, Ibaraki 305, Japan

A detailed study of the microstructures and superconducting properties of the *in situ* V_3Ga prepared by external gallium diffusion has been carried out. The structure of the final reacted layer has been found to be divided into two regions: an outer layer composed of multiple connected V_3Ga globules and an inner layer composed of filamentary V_3Ga surrounded by a Cu–Ga matrix. The particle-like V_3Ga in the outer region has a slightly higher T_c and, hence, higher H_{c2} than the filamentary V_3Ga in the inner region. Therefore, it should be recognized that the measured I_c is a combined contribution from both regions having a different magnetic field dependence of J_c. I_c at high magnetic field is primarily contributed by the outer region. The I_c anisotropy of the tape conductor results from the anisotropic shape of filamentary V_3Ga in the inner region. The highest overall J_c obtained is $\sim 2 \times 10^5$ A cm^{-2} at 12.5 T. Further optimization based on the microstructural control, which can be achieved by the appropriate design of the process, may yield *in situ* V_3Ga composites having substantially improved properties.

1. Introduction

The *in situ* prepared A15 filamentary composites have become of technological interest due to their simplicities in process and superior mechanical properties. In an earlier study, the direct casting and subsequent cold-working of a Cu–V–Ga(Cu–Nb–Sn) ternary alloy has been utilized, where only the gallium(tin) contained in the starting ingot contributes to the formation of $V_3Ga(Nb_3Sn)$ in the final reaction. This method, however, has a limitation in the amount of gallium(tin) additive in order to allow sufficient workability of the ingot for fabrication into a thin tape without any intermediate annealing. Recently, the "external diffusion method", which was originally introduced in the fabrication of Nb_3Sn multifilamentary wire from a composite of niobium cores in a pure copper matrix, was applied to the *in situ* processes $V_3Ga(Nb_3Sn)$ composite, resulting in a significant improvement of superconducting properties such as overall critical current density, J_c [1].

From investigation of the conventional multifilamentary Nb_3Sn conductor prepared by the "external diffusion method", several difficulties accompanying external diffusion have been revealed:

1. a non-uniform amount of tin plating would directly cause inhomogeneous superconducting properties in the longitudinal direction of the resulting composite [2];

2. the molten tin layer dewets the copper and tends to "ball-up" in the early stages of reaction, resulting in an island of very high tin concentration in the final reacted composites, which would make the composite extremely brittle and decrease J_c catastrophically [3];

3. Kirkendall porosity forms near the surface of the composite and introduces a resistance to further diffusion of tin, which would lead to the separation of a tin-rich outer layer [4].

These macrostructural phenomena, as well as the microstructural changes accompanied with external diffusion of tin, have been investigated in

0022–2461/84 $03.00 + .12

detail for the *in situ* Nb_3Sn composite [5, 6]. However, there has been only a little information about the metallurgical aspects of the *in situ* V_3Ga composite prepared by the external diffusion method. For this reason, an extensive investigation of the structural changes of the *in situ* V_3Ga composite during external diffusion of gallium has been carried out using X-ray diffraction, X-ray microprobe analysis (XMA) and scanning electron microscopy (SEM). In this paper, some observed phenomena peculiar to the *in situ* V_3Ga composite are given and correlated with the superconducting properties such as transition temperature T_c, critical current I_c, and the I_c anisotropy in the tape conductor.

2. Experimental procedure

Cu–(30, 35, 40) at % V binary alloy ingots (40 mm diameter) were prepared by consumable electrode arc melting as described in detail elsewhere [1], where a laminated composite, consisting of copper and vanadium plates, was used as an electrode. The purities of the starting materials were 99.99 and 99.8 at %, respectively. A quite uniform distribution of fine vanadium dendrites ($\sim 10\,\mu m$) without any undissolved vanadium particles could be attained by arc melting once only, because of the large contact area between copper and vanadium in the electrode. The ingots were then cold-worked into wires (0.2 and 0.3 mm diameter) and various size tapes (~ 0.1 mm thick). The ratio of initial cross-sectional area to final area of the tape composite was 3.5×10^3 (for example, 0.11 thickness × 3 wide mm tape), which was considerably smaller than that of the 0.2 mm diameter wire of 3.6×10^4. Several samples were subjected to annealing at 800° C for 1 h prior to gallium dipping, which is the designated pre-heat-treatment in the present paper, in order to investigate the effects of vanadium filament morphology on the gallium diffusion and the anisotropic properties in I_c of the tape conductors. The tapes and wires were then continuously coated with gallium by passing them through a molten gallium bath. The dipping apparatus was essentially the same as that utilized for preparing the surface-diffusion processed V_3Ga tape [7]. The amount of additive gallium could be easily controlled by varying the molten gallium bath temperature between 400 and 500° C and/or the moving speed of the composite from 0.2 to 1.3 m min^{-1} (corresponding to a dipping time of 48 to 7.4 sec). Subsequently, the dipped composite was preliminary heat-treated at 500° C for a few minutes through the two pipe-shaped furnaces. Sections of these dipped composites were encapsulated in quartz tubes and finally heat-treated for various times at temperatures between 450 and 700° C.

XMA was performed to obtain the compositional profiles on the cross-section of the tape composite at various stages of gallium diffusion. The X-ray diffraction on the surface of the tape was also performed to identify the V–Ga and Cu–Ga compounds which were formed during gallium diffusion. The changes of vanadium and V_3Ga filaments morphology and configuration were studied by SEM. Samples for SEM observation were prepared by selectively etching away the copper or Cu–Ga alloy on the polished cross-section of the composite in dilute nitric acid. The ribbon-like vanadium filaments of the as-rolled Cu–V tape, which align parallel to the tape surface, tend to contact each other after etching away the copper matrix, masking the true morphology and configuration of the filaments. This can be avoided by annealing the tape at a low temperature of 300° C for 1 h prior to etching, which minimizes the excessive etching at the interface between vanadium filament and copper matrix.

I_c was measured at 4.2 K in transverse steady magnetic fields up to 21 T. An angular dependence of I_c of the tape in the transverse magnetic field was characterized by the ratio $I_c(\theta)/I_{c,\perp}$ where θ was the angle between the tape surface and magnetic field direction (Fig. 9). The magnetic field dependence of the anisotropic factor, defined in this paper as the ratio $I_{c,\parallel}/I_{c,\perp}$, was measured over the field range 3 to 16 T.

3. Metallurgical microstructures

3.1. Vanadium filaments

Fig. 1 shows scanning electron micrographs of the transverse cross-section of the Cu–V composite wire and tape, which reveal differences in the vanadium filament morphology and configuration. In the as-drawn wire, ribbon-like filaments of vanadium are curled and randomly oriented (Fig. 1a), while in the as-rolled tape, the filaments are relatively flat and aligned parallel to the rolling plane (Fig. 1b). Similar differences were reported for the *in situ* Cu–Nb wire and tape [8]. The ribbon-like shape with high aspect ratio is unstable because of the large interfacial area and tends to change to a shape with lower aspect ratio at

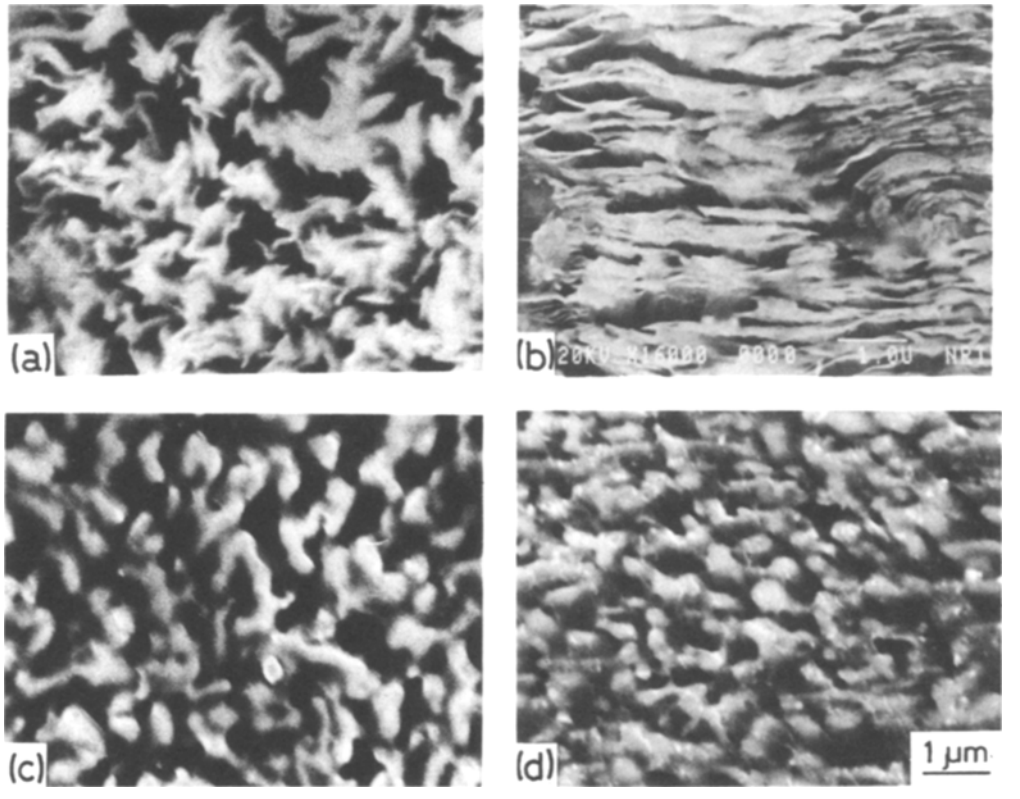

Figure 1 Typical SEM photographs of polished and etched transverse cross-section of the *in situ* Cu–V binary composite. (a) as-drawn wire, (b) as-rolled tape, (c) (d) wire and tape pre-heated at 800° C for 1 h, respectively.

elevated temperatures. Figs. 1c and d show the micrographs after pre-heat-treatment at 800° C for 1 h, which indicate a significant morphological change to a nearly cylindrical shape for both the wire and tape composites. The morphological change is also observed in the longitudinal direction of the filament. Fig. 2 shows the longitudinal view of vanadium filaments in the *in situ* Cu–V tape annealed at 800° C for 1 h. The straight ribbon-like filament is found to have broken up into columns of connected cylindrically shaped granules. Similar phenomena of morphological instabilities of the fibrous phase in the various alloys have been recently reviewed by McLean [9].

3.2. Reaction with gallium and microstructures

Fig. 3 shows the compositional profiles of the cross-section of the *in situ* Cu–V tape dipped in a molten gallium bath at 500° C. A few gallium-diffused layers were formed near the surface of the tape. The total thickness of these gallium-diffused layers is considered to be an important parameter which represents roughly the amount of gallium. The thickness is strongly influenced by the dipping parameters, the vanadium concentration and the filament morphology as follows [10]:

1. total thickness of the gallium-diffused layers, that is, additive amount of gallium, increases with

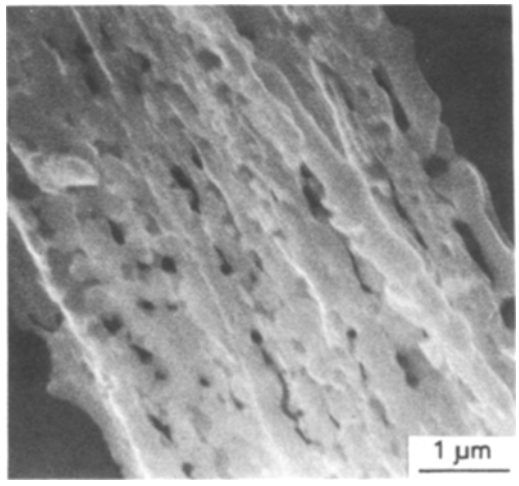

Figure 2 Longitudinal view of vanadium filaments in the *in situ* Cu–V binary tape, pre-heated at 800° C for 1 h.

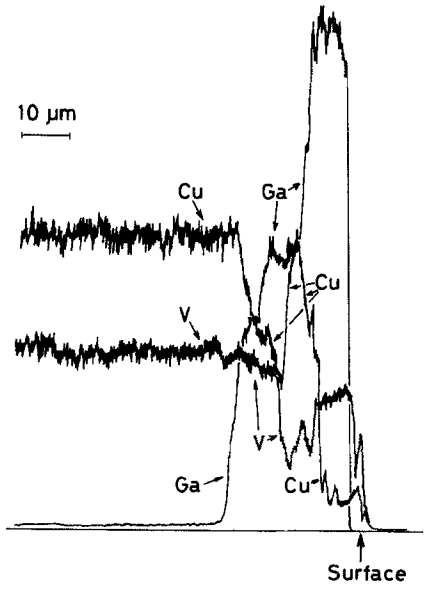

Figure 3 Compositional profiles of the cross-section of the *in situ* Cu–V tape dipped in a molten gallium bath at 500° C for 16 sec.

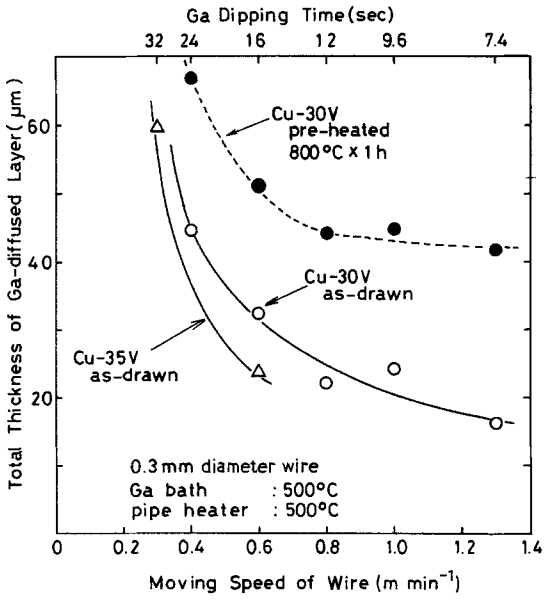

Figure 4 Total thickness of gallium-diffused layers as a function of the moving speed of wire through the gallium bath held at 500° C.

increasing gallium bath temperature and decreasing moving speed of the tape through the gallium bath;

2. the increase in vanadium concentration in Cu–V composite decreases the thickness, and, for a given vanadium concentration, pre-heat-treatment which causes the morphological change in vanadium filament increases the thickness;

3. the layers are thinner in the tape sample than in the wire sample. Fig. 4 shows an example of the variation of total thickness as a function of moving speed of the wire through the gallium bath held at 500° C. The results clearly indicate the influences of vanadium concentration and pre-heat-treatment.

Fig. 5 shows a typical scanning electron micrograph of a polished and etched longitudinal cross-section of the as-dipped tape sample. Gallium-rich compound layers indicated by XMA (Fig. 3) correspond to the right-hand (outer) region where the ribbon-like vanadium filaments have broken up into a multiply connected discrete structure of small compound globules, while the unreacted vanadium filaments in the extreme left region have scarcely changed in morphology during the dipping process at 500° C. This breaking up of filament due to the reaction with gallium seems to be essentially the same as the morphological instability of pure vanadium filament which occurs at higher temperatures (Fig. 2). The breaking up is more significant in the layer with higher gallium concentration, which suggests that gallium promotes the breaking up of the ribbon-like filament through the formation of a gallium-rich compound. This is because the melting point of the gallium-rich compounds is lower than that of pure vanadium.

Identification of these gallium-rich compounds was performed using an X-ray diffraction technique, and the results are summarized in Table I. For the as-dipped tape, all peaks of the diffraction pattern from the surface were completely iden-

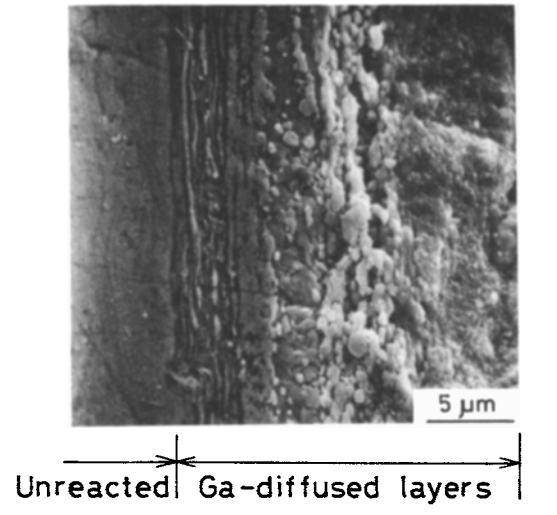

Figure 5 Typical SEM photograph of polished and etched longitudinal cross-section perpendicular to the rolling plane for the as-dipped tape.

TABLE I Results of X-ray diffraction analysis on various tapes

Vanadium concentration in Cu–V tape (at %)	Dipping time at 500° C (sec)	Heat-treatment time at 500° C (h)	Observed phases	
30	16	–	V_2Ga_5	strong
			φCuGa	strong
			V_6Ga_5	weak
30	16	– (hand-polished)	V_2Ga_5	weak
			φCuGa	strong
			V_6Ga_5	strong
30	16	10	δCu_9Ga_4	strong
			V_6Ga_5	trace
			V_3Ga	weak
30	16	100	Cu–Ga (fcc)	strong
			V_3Ga	medium
30	24	100	Cu–Ga (fcc)	trace
			δCu_9Ga_4	strong
			V_3Ga	medium
35	24	100	Cu–Ga (fcc)	strong
			V_3Ga	medium

tified as those of V_2Ga_5, φCuGa and V_6Ga_5. Although no peak of bcc vanadium was observed in the diffraction pattern, it is still unknown whether the globules in the diffusion layers have completely reacted with gallium or if the unreacted core of vanadium remains in the compound globule. Removal of the outermost layer by hand-polishing the tape surface resulted in a decrease in relative intensity of the V_2Ga_5 peak to the V_6Ga_5 peak, indicating that V_6Ga_5 has located in the interior. Taking account of the XMA result, it is concluded that the outermost layer consists of V_2Ga_5 globules and the surrounding φCuGa matrix. It is, here, interesting to consider why the *in situ* composite can be successfully added with sufficient gallium by the hot dipping process. In the case of the external diffusion method for conventional multifilamentary wire, the hot dipping process results in a removal of the copper matrix, because copper easily dissolves into a molten gallium bath. The success in the dipping process for the *in situ* composite is attributed to the formation of interconnected V_2Ga_5 globules which act as a support for the semimolten Ga–Cu compounds. Table I also reveals that a subsequent reaction heat-treatment at 500° C decomposes the gallium-rich compounds formed near the surface (V_2Ga_5, φCuGa) into lower gallium concentration compounds (V_6Ga_5, δCu_9Ga_4) and finally converts them into V_3Ga and Cu–Ga fcc solid solution. δCu_9Ga_4 phase sometimes remains as matrix material on the tape surface even after the final heat-treatment of 500° C for 100 h, when gallium is added in excess, for instance, by dipping the Cu–V tape at relatively slow moving speeds. The existence of δCu_9Ga_4 on the final tape surface is undesirable, because it leads into brittleness of the resulting composite. However, an increase in vanadium concentration, which leads into a decrease in amount of gallium additive as mentioned previously, suppresses the appearance of the δCu_9Ga_4 phase after the final reaction.

Fig. 6 shows the compositional profiles on the cross-section of finally reacted *in situ* V_3Ga tape.

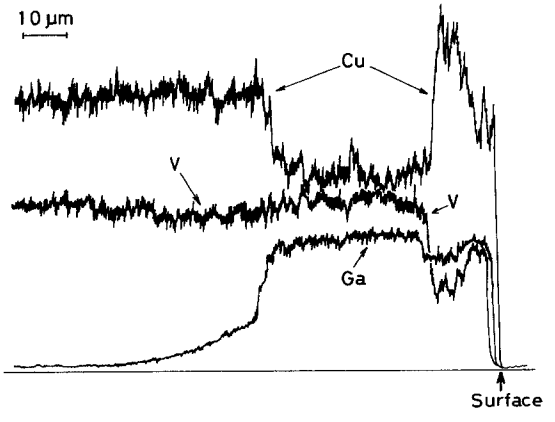

Figure 6 Compositional profiles on the cross-section of finally reacted *in situ* V_3Ga tape at 500° C for 100 h.

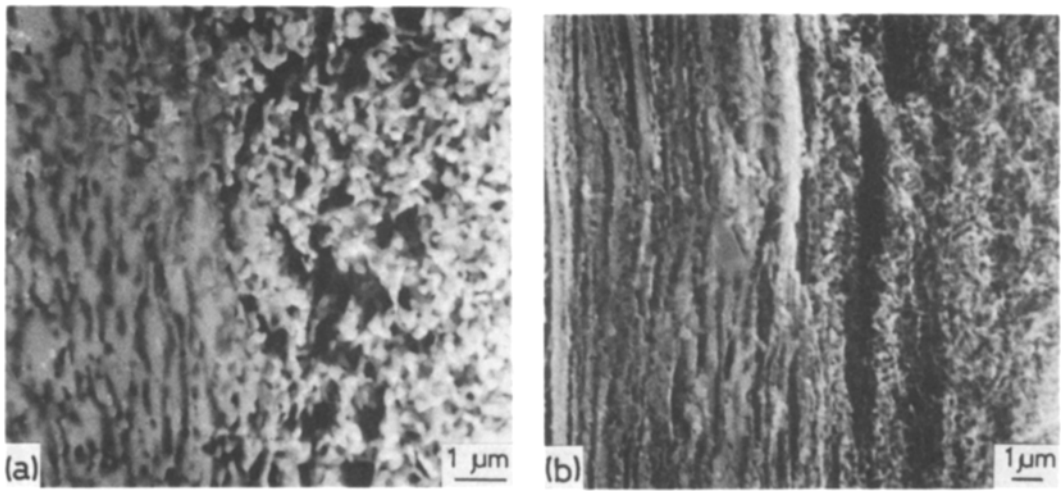

Figure 7 Typical SEMs of polished and etched cross-section of the finally reacted *in situ* V_3Ga tape at 500° C for 100 h. (a) transverse, (b) longitudinal.

From comparison with the compositional profiles of the as-dipped tape (Fig. 3), it is easily seen that the gallium-rich compounds formed near the surface have been decomposed and the gallium has diffused further inward. In the outer region, where gallium-rich compounds were located before the final reaction, the copper concentration becomes higher than that in the inner region, while gallium and vanadium concentrations seem to be rather lower. X-ray diffractions performed on the as-reacted tape surface and the subsequently hand-polished tape surface revealed that the lattice parameter of A15 V_3Ga in the outer region was essentially the same as in the inner region. The gallium concentration in the Cu–Ga solid solution can be qualitatively estimated by the magnitude of the increase in lattice parameter from the value of pure copper. The increment is rather small for the outer region, indicating that the gallium concentration in the Cu–Ga solid solution is considerably lower in the outer region than in the inner region. This is consistent with the concentration profile of copper in Fig. 6 showing a lower level at the inner region. These results suggest a kind of "uphill" diffusion for gallium, which is not observed for the external diffusion of gallium to pure copper matrix. The "uphill" diffusion is well known to occur in a multiple component alloy system such as Fe–Si–C [11], where the carbon diffuses down a gradient in the chemical potential of carbon which is contrary to a gradient in the concentration. A similar phenomenon was reported for Cu–Sn–Ga ternary alloy where gallium was introduced into the Cu–Sn binary alloy by external diffusion [12, 13].

Typical scanning electron micrographs of the transverse and longitudinal cross-section of the finally reacted *in situ* V_3Ga tape are shown in Figs. 7a and b, respectively. As expected from the results of the compositional profiles, the gallium-diffused region can be divided into two parts. In the outer region (right-hand side), the filamentary structure is completely lost, and an almost isotropic particle-like V_3Ga multiply connects with each other and forms a three-dimensional network. The average size of the particle-like V_3Ga is about 200 nm, which is smaller than the grain size of V_3Ga prepared by the conventional bronze process [14]. SEM observation for the sample reacted for a shorter time (5 h) revealed that this network was formed in the early stage of the final reaction at which point gallium-rich compounds had not yet decomposed. On the other hand, in the inner region (left-hand side), the filamentary structure remains unchanged, although the filament has coarsened slightly. This is due to the direct conversion of the vanadium filament into V_3Ga, and not through an intermediate compound with lower melting point. The aspect ratios of the filamentary V_3Ga in this region are typically in the range 5 to 20. The ratio of the thickness of the particle-like V_3Ga region to that of the filamentary V_3Ga region increases with initial thickness of the gallium-rich compound layers. Annealing prior to the dipping process, which causes coarsening of vanadium filaments

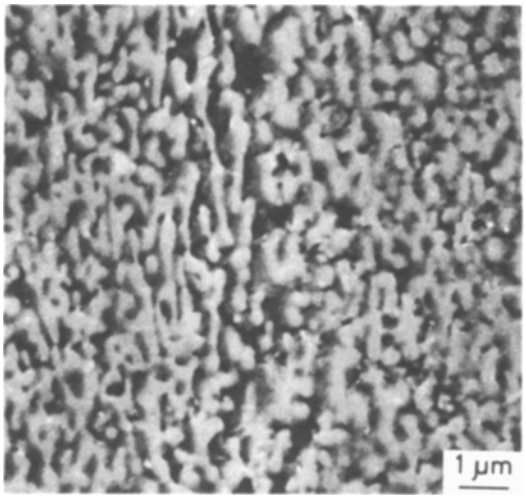

Figure 8 Typical SEM of polished and etched transverse cross-section of finally reacted *in situ* V_3Ga tape which have been pre-heated prior to the dipping process.

(Fig. 1), suppresses the break up of the filaments during the reaction with galloum. In fact, the difference in the two kinds of V_3Ga microstructure has become unclear, as shown in Fig. 8. This is because the driving force for the morphological instabilities, that is, the interfacial energies between vanadium filament and copper matrix, was reduced by annealing prior to the reaction with gallium.

In order to compare the microstructural change of the *in situ* Nb_3Sn with that of V_3Ga, we prepared the *in situ* Cu–30 at % Nb tape and introduced tin by electroplating and subsequent heat-treatment. X-ray diffraction analysis and SEM observation revealed that the niobium filament near the surface was converted into a tin-rich compound of Nb_6Sn_5 after reaction at 550° C for 100 h, but that the filamentary structure remained unchanged. For the *in situ* Nb_3Sn composite. $NbSn_2$ (which is well known as the most tin-rich intermetallic compound in the Nb–Sn binary phase diagram) is considered to have been formed in the early stage of tin diffusion from the analogy to the formation of V_2Ga_5 for the *in situ* V_3Ga composite. The melting point of V_2Ga_5 (1358 K) is higher than that of $NbSn_2$ (1118 K) reported in each binary phase diagram [15, 16]. However, it is considered that the copper is much more easily incorporated into V_2Ga_5, significantly lowering its melting point. This was also suggested by Tanaka for the surface-diffusion processed V_3Ga tape as a reason for the enhancement of V_3Ga growth rate by copper addition [17]. Therefore, the absence of break up of filaments for $NbSn_2$ is probably due to its higher melting point than that of V_2Ga_5, because only a few per cent of copper is incorporated into $NbSn_2$ [18]. This difference in morphology between V_2Ga_5 and $NbSn_2$ is reponsible for the morphological difference between granular V_3Ga and filamentary Nb_3Sn in each outer region observed after the final reaction.

4. Anisotropy in I_c

The *in situ* V_3Ga shows pronounced anisotropy in I_c. Fig. 9 demonstrates an angular dependence of the normalized critical current $I_c(\theta)/I_{c,\perp}$ at 12.5 T, where θ is an angle between the applied magnetic field and the tape surface. It is easily found that the strongest pinning occurs when the fluxoids are parallel to the tape surface. This is contrary to the result for the conventional bronze-processed V_3Ga tape in which $I_{c,\perp}$ is appreciably larger than

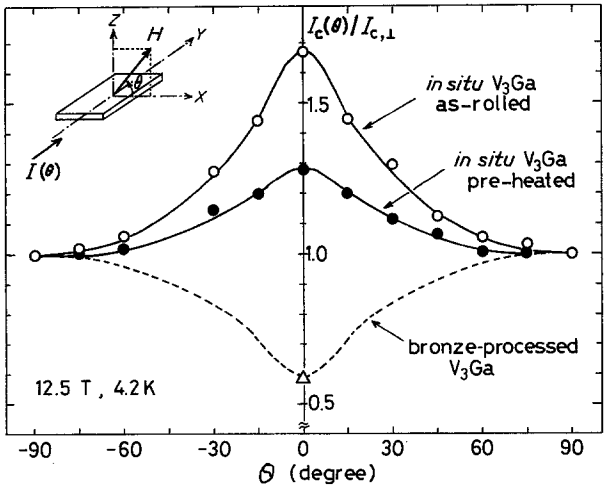

Figure 9 Angular dependence of normalized I_c for V_3Ga tape.

TABLE II Critical current and anisotropy factor for the Cu–40 at % V tape ($0.11^{t} \times 3^{w}$ mm) dipped and subsequently heat-treated at various conditions

Ga dipping condition		Ga-diffused layer thickness (μm)	Final heat-treatment		$I_{c,\parallel}$ at 12.5 T (A)	$I_{c,\perp}$ at 12.5 T (A)	$I_{c,\parallel}/I_{c,\perp}$ at 12.5 T
(m min^{-1})	(°C)		(°C)	(h)			
0.2	500	30	500	100	320	343	0.93
0.4	500	23	500	100	443	357	1.24
0.6	500	18	500	100	468	360	1.30
1.0	500	15	500	100	250	166	1.50
1.0	450	8	500	100	176	100	1.76
1.0	500	15	500	100	250	166	1.50
1.0	500	15	600	100	138	95	1.45
1.0	500	15	650	100	61	47	1.30
1.0	500	15	700	100	0.39	0.43	0.90

$I_{c,\parallel}$, as shown by the broken line in Fig. 9. The I_c anisotropy of the *in situ* tape seems to be advantageous to the stability of superconducting magnet. In the bronze-processed V_3Ga tape, grain boundaries are major flux-pinning centres, and the anisotropy in I_c is interpreted as a result of the columnar grain growth of V_3Ga in the direction perpendicular to the tape surface [14]. The interfaces between superconductive V_3Ga and the normal-conductive Cu–Ga matrix, which can act as stronger pinning centres than the grain boundaries, do not play an important role in anisotropy in I_c in the bronze-processed V_3Ga composite, because thetotal area of the interface per unit volume is much smaller than that of the grain boundary. On the other hand, in the *in situ* composite tape, the filament size becomes comparable to the grain size [6] so that surface pinning by filament–matrix interface contributes significantly to the total pinning force [19]. Therefore, it is considered that the highest I_c in the parallel magnetic field results from the parallel alignment of the filament–matrix interface with high aspect ratio to the tape surface, as presumed by Bevk *et al.* for the *in situ* Nb_3Sn tape [8]. However, for the *in situ* V_3Ga tape, the alignment of the filament–matrix interface remains only in the inner region, and the particle-like V_3Ga in the outer region may not be responsible for the anisotropy behaviour of I_c because of its isotropic morphology, as shown in Fig. 7. It is considered that the two regions have different current capacities and a measured critical current (total current) for the *in situ* V_3Ga tape, $I_{c,\text{total}}$, is the sum of the critical current in the inner region, $I_{c,\text{inner}}$, and that in the outer region, $I_{c,\text{outer}}$, as follows:

$$I_{c,\text{total}} = I_{c,\text{inner}} + I_{c,\text{outer}}$$

The anisotropy factor of the whole tape should be given by

$$\alpha_{\text{total}} = \frac{I_{c,\text{total},\parallel}}{I_{c,\text{total},\perp}} = \frac{I_{c,\text{inner},\parallel} + I_{c,\text{outer},\parallel}}{I_{c,\text{inner},\perp} + I_{c,\text{outer},\perp}}$$

where

$$I_{c,\text{outer},\parallel} \sim I_{c,\text{outer},\perp}$$

Table II summarizes the critical current in the parallel and perpendicular magnetic fields and the anisotropy factor for the Cu–40 at % V tape dipped and subsequently heat-treated at various conditions. The anisotropy factor, for a given dipping condition, decreases with increasing final reaction temperature. This is because the coarsening of V_3Ga filaments in the inner region, which is accompanied by the reduced aspect ratio of the filament, is more significant at high reaction temperatures. The anisotropy factor, for a given heat-treatment condition, is varied by dipping condition, and can be arranged in magnitude according to the total thickness of gallium-rich compound layers formed just after the dipping process. As mentioned in the previous section, this thickness corresponds to that of the particle-like V_3Ga region formed after the final reaction. Therefore, the increase in this thickness enhances the contribution of $I_{c,\text{outer}}$ to $I_{c,\text{total}}$ and leads to a decrease of the anisotropy in $I_{c,\text{total}}$. Anisotropy is also measured for the pre-heated *in situ* V_3Ga tape and found to be reduced by the pre-heat-treatment (Fig. 9). This result agrees with the microstructure of the low aspect ratio V_3Ga filament as shown in Fig. 8, which is due to the morphological change of vanadium filament prior to the reaction with gallium.

The coexistence of two reaction layers with different V_3Ga morphology is also responsible

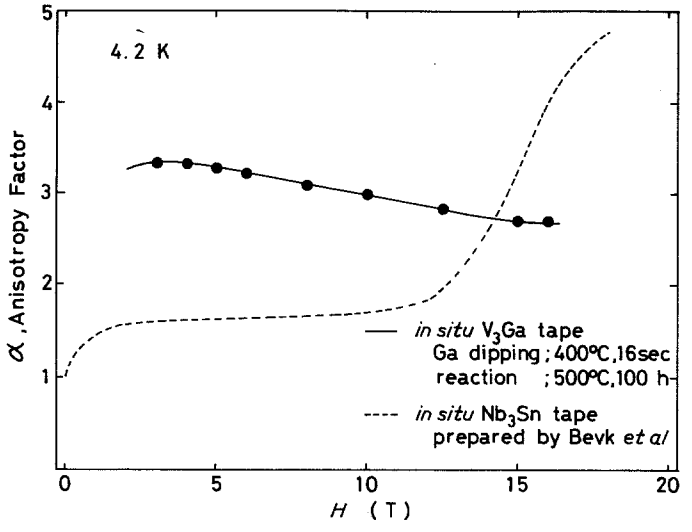

Figure 10 Magnetic field dependence of the anisotropy factor for the *in situ* V_3Ga and Nb_3Sn [8] tape.

for the magnetic field dependence of anisotropy peculiar to the *in situ* V_3Ga tape. As shown in Fig. 10, the anisotropy factor of the *in situ* V_3Ga tape gradually decreases with increasing magnetic field. This is in contrast to the result for the *in situ* Nb_3Sn tape in which the anisotropy increases with increasing magnetic field. The rapid increase in anisotropy factor in high fields for the *in situ* Nb_3Sn tape was explained as being due to the anisotropy in the upper critical magnetic field H_{c2} from the analogy to the transport behaviour of *in situ* Cu–Nb binary alloy tapes [8, 20]. Considering the similarity in the morphology and configuration between V_3Ga filament in the inner region and Nb_3Sn filament, the anisotropy in $I_{c,inner}$ is considered to increase with magnetic field, which is not consistent with the observed anisotropy at least up to 16 T. However, if the degradation of $I_{c,outer}$ with magnetic field is smaller than that of $I_{c,inner}$, the contribution of $I_{c,outer}$ to $I_{c,total}$ is increased with increasing magnetic field, resulting in a reduction of anisotropy in $I_{c,total}$ at high magnetic fields. This occurs if the T_c, hence, H_{c2} of V_3Ga in the outer region is higher than that in the inner region.

In order to confirm the above speculation, T_c of an *in situ* V_3Ga tape was measured by the induction method. Fig. 11 shows a temperature dependence of the normalized susceptibilities χ of the *in situ* V_3Ga tape in parallel and perpendicular magnetic fields, where both of the tape side edges were planed off to expose the inner region to external magnetic fields. A two-stage transition is clearly observed both in the parallel and perpendicular magnetic fields, indicating the co-existence of V_3Ga phases with slightly different T_c. If the higher T_c phase is located in the inner region, the susceptibility change, $\Delta\chi$, remains unchanged irrespective of the magnetic field direction. However, the observed susceptibility change, $\Delta\chi$, at the higher temperature becomes smaller in the parallel magnetic field, indicating that the higher T_c phase

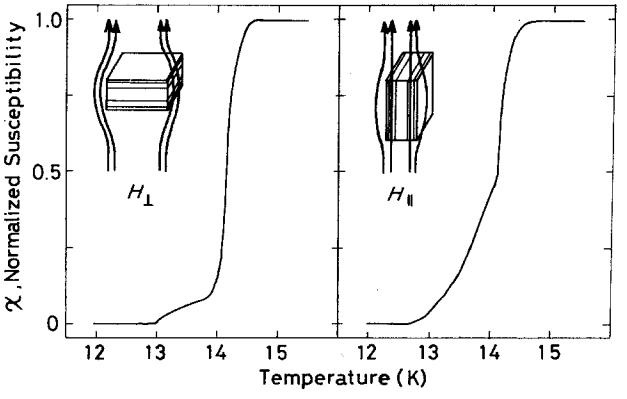

Figure 11 Temperature dependence of the normalized susceptibility of the *in situ* V_3Ga tape in parallel and perpendicular magnetic fields.

is located outside. Therefore, it is concluded that the particle-like V_3Ga in the outer region has a higher T_c and, hence, higher H_{c2} than the filamentary V_3Ga in the inner region. It is difficult to give a substantial account of the origin of the different superconducting properties, but it may be related to the different mechanisms of V_3Ga formation. The V_3Ga in the inner region is formed by the solid-state reaction between vanadium and Cu–Ga solid solution just as in the conventional bronze process, while the V_3Ga in the outer region is converted from gallium-rich compounds by the catalytic action of copper. The latter is similar to the conventional surface diffusion process for V_3Ga. Tanaka *et al.* actually reported that the H_{c2} of the bronze-processed V_3Ga is slightly lower than that of the surface diffusion processed V_3Ga [21], the difference being considered to result from the same origin as in the present study.

5. Critical current

As mentioned in the previous section, critical current I_c (overall J_c) of the *in situ* V_3Ga tape varies with the microstructure of composite. The highest J_c is obtained at the final reaction temperature of 500° C (Table II). The reduced J_cs at higher reaction temperatures are due to a combination of reduced V_3Ga–matrix interfacial area and increased grain size of V_3Ga, both of which are accompanied by the coarsening filaments and particles of V_3Ga. Table II also indicates that the overall J_c strongly depends on the dipping condition. We previously reported that the optimum dipping condition for overall J_c varies with microstructure of the vanadium filament such as volume fraction, configuration and morphology through the diffusivity of gallium in the Cu–V composite [10]. Fig. 12 shows the plot of overall J_c against parallel magnetic field, $H_{\parallel}$, of the *in situ* V_3Ga tape and wire finally reacted at 500° C for 100 h. The 0.2 mm diameter wire shows a slightly higher J_c than those of the tapes at the entire magnetic field. This is probably due to the larger area reduction and the different conductor morphology which leads to the different diffusion kinetics of gallium during the reaction. The highest overall J_c at 12.5 T is $\sim 2 \times 10^5$ A cm^{-2}, which is significantly higher than the best value of commercial multifilamentary V_3Ga wires [22]. The extrapolated H_{c2} at 4.2 K is about 21.5 T. Further research based on the microstructural control is expected to yield *in situ* V_3Ga composites having substantially improved superconducting properties.

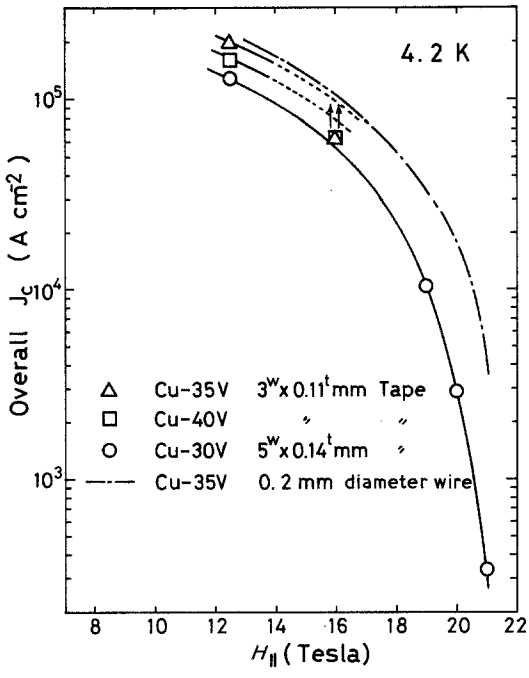

Figure 12 Overall J_c plotted against parallel magnetic field, $H_{\parallel}$, for the *in situ* V_3Ga wire and tape conductors. J_c was measured in magnetic fields of 12.5, 12.5 to 16 and 16 to 21 T using 13 T (Nb–Ti)–V_3Ga and 17.5 T Nb_3Sn–V_3Ga hybrid superconducting magnets at NRIM and a Bitter type hybrid magnet at Francis Bitter National Laboratory of MIT, respectively.

6. Conclusions

1. Gallium-rich compound layers consisting of V_2Ga_5, φCuGa, etc, are formed on the surface of the *in situ* Cu–V composite during a continuous dipping process. Ribbon-like filaments aligned parallel to the rolling plane in the as-rolled Cu–V composite tape break up into a multiply connected discrete structure of small compound globules in this process.

2. The final gallium-diffused region is revealed to consist of two parts where reacted V_3Ga is different in morphology and configuration. In the outer region, isotropic particle-like V_3Ga interconnects and forms a three-dimensional network, while in the inner region, the filamentary structure remains unchanged and the aspect ratios of the filamentary V_3Ga are in the range 5 to 20.

3. The break up of filamentary structure is not appreciable for the *in situ* Nb_3Sn. This is probably due to the initially formed $NbSn_2$ being more

stable than V_2Ga_5 because less copper can be incorporated within the $NbSn_2$.

4. The particle-like V_3Ga in the outer region has a higher T_c than the filamentary V_3Ga in the inner region.

5. The *in situ* V_3Ga shows a pronounced anisotropy in I_c. $I_{c,\parallel}$ is larger than $I_{c,\perp}$, which is contrary to the result for conventional bronze-processed tape. The anisotropy of the *in situ* V_3Ga, resulting from the aligned filamentary structure of V_3Ga in the inner region, is reduced by pre-heat-treatment and higher reaction temperature. The dependence of the anisotropy on the dipping condition and magnetic field is correlated with the co-existence of two reaction layers with different V_3Ga morphology.

6. The highest overall $J_{c,\parallel}$ of $\sim 2 \times 10^5$ A cm^{-2} at 12.5 T is obtained for the Cu–35 at% V tape ($0.11^t \times 3^w$ mm), which is comparable to that of the 0.2 mm diameter wire. Anisotropy in I_c seems to be advantageous to the *in situ* V_3Ga tape conductor utilized for an insert magnet.

Acknowledgements

The authors would like to thank Mr H. Araki and Dr H. Kawamura of the National Research Institute for Metals (NRIM) for the XMA operation and for the T_c measurement by the induction method, respectively. They are also indebted to Mr H. Kumakura of the NRIM for the J_c measurement at 17 to 21 T using a Bitter-type magnet of the Massachusetts Institute of Technology.

References

1. H. KUMAKURA, K. TOGANO and K. TACHIKAWA, *Adv. Cryogenic Engng (Mater.)* **28** (1982) 515.
2. M. SUENAGA, W. B. SAMPSON and C. J. KLAMUT, *IEEE Trans. Mag.* **MAG-11** (1975) 231.
3. J. D. VERHOEVEN, E. D. GIBSON and C. C. CHENG, *Appl. Phys. Lett.* **40** (1982) 87.
4. S. COGAN, D. S. HOLMES and R. M. ROSE, *ibid.* **35** (1979) 557.
5. R. ROBERGE, in "Superconducting Materials Science", Vol. B68, edited by S. Forner and B. B. Schwartz, (Plenum, New York, 1981) Ch. 6, p. 389.
6. L. D. VERHOEVEN, J. J. SUE, D. K. FINNEMORE, E. D. GIBSON and J. E. OSTENSON, *J. Mater. Sci.* **15** (1980) 1907.
7. S. FUKUDA, K. TACHIKAWA and Y. IWASA, *Cryogenics* **13** (1973) 153.
8. J. BEVK, M. TINKHAM, F. HABBAL, C. J. LOBB and J. P. HARBISON, *IEEE Trans. Mag.* **MAG-17** (1981) 235.
9. M. MCLEAN, *Met. Sci.* **12** (1978) 113.
10. T. TAKEUCHI, K. TOGANO, H. KUMAKURA and K. TACHIKAWA, in Proceedings of the International Cryogenic Materials Conference, Kobe, May 1982, edited by K. Tachikawa and A. Clark (Butterworth, Surrey, 1982) p. 323.
11. L. DARKEN, *Trans. AIME* **180** (1949) 430.
12. S. KWON, S. F. COGAN, J. D. KLEIN and R. M. ROSE, *J. Appl. Phys.* **54** (1983) 1008.
13. H. SEKINE, T. TAKEUCHI and K. TACHIKAWA, *IEEE Trans. Mag.* **MAG-17** (1981) 383.
14. Y. TANAKA, K. ITOH and K. TACHIKAWA, *J. Jpn. Inst. Met.* **40** (1976) 515.
15. J. P. CHARLESWORTH, I. MACPHALL and P. E. MADSEN, *J. Mater. Sci.* **5** (1970) 580.
16. J. H. N. van VUCHT, H. A. C. M. BRUNING, H. C. DONKERSLOOT and A. H. GOMES de MESQUITA, *Philips Res. Rept.* **19** (1964) 407.
17. Y. TANAKA, K. TACHIKAWA and K. SUMIYAMA, *J. Jpn. Inst. Met.* **34** (1970) 835.
18. U. ZWICKER and L. RINDERER, *Z. Metallkde* **66** (1975) 738.
19. J. BEVK, J. P. HARBISON, F. HABBAL, G. R. WAGNER and A. I. BRAGINSKI, *Appl. Phys. Lett.* **36** (1980) 85.
20. F. HABBAL, K. R. KARASEK and J. BEVK, to be published.
21. Y. TANAKA and K. TACHIKAWA, *J. Jpn. Inst. Met.* **40** (1976) 509.
22. Y. FURUTO, T. SUZUKI, K. TACHIKAWA and Y. IWASA, *Appl. Phys. Lett.* **24** (1974) 34.

Received 9 September
and accepted 29 September 1983